Kinetics of Spinodal Decomposition in Liquid Crystalline Polymers: Processing Effects on the Phase Separation Morphology

John R. Dorgan* and Dong Yan

Chemical Engineering and Petroleum Refining Department, Colorado School of Mines, Golden, Colorado 80401

Received August 7, 1997; Revised Manuscript Received October 30, 1997

ABSTRACT: Results from a Landau−Ginzburg model which treats the problem of spinodal decomposition of liquid crystalline polymers (LCPs) in solution are presented. Morphological evolution of one conserved order parameter (polymer volume fraction) and one nonconserved order parameter (the Flory orientational order parameter) is considered. Processing effects on morphology including quench temperature, composition, solvent quality, and molecular weight are presented. Simulations of example quenching experiments demonstrate that increased LCP concentration, decreased molecular weight, increased solvation, and decreased quench depth all lead to increased domain size. Implications of the model regarding the optimization of processing conditions for LCP fiber spinning and film casting are discussed.

Introduction

Liquid crystalline polymers (LCPs) are a unique class of materials. Due to their rigid structure a high degree of molecular orientation can be achieved during processing, thereby leading to extraordinary properties. Fibers made from LCPs are among the strongest materials known to mankind with respect to tensile properties on a per unit weight basis.[1] Unfortunately, compressive properties are limited and LCP fibers will buckle under relatively low loading. For example, in PBT (poly[*p*-phenylene(benzo[1,2-*d*:4,5-*d′*]bisthiazole-2,6-diyl)]) tensile moduli of 300 GPa and tensile strengths of 3 GPa are reported[2,3] but the compressive strength is only about 0.3 GPa.[4]

The mechanism of this compressive failure is complex but is at least partially attributable to failure at the microfibrillar interfaces within the fiber.[5] These microfibrils form as a result of the flow and deformation of liquid crystalline domains during processing into fibers or films. Domains are formed during a phase separation process which takes place either as a result of coagulation (in the case of a lyotropic material) or because of cooling (in the case of thermotropic LCPs). The interfacial area of the microfibrils can be minimized through an understanding of how the system parameters (molecular weight, concentration, temperature, and solvent quality) affect the phase-separated morphology.

LCPs and their oligomeric counterparts are also finding increased use in electrical and optical applications.[6] These applications require careful control of the morphological properties of the liquid crystalline materials, oftentimes in the presence of an interface. Despite the structural and electronic applications for LCPs, relatively little theoretical work is available for guiding the processing of these materials into useful articles.

Background

One electro-optical application of liquid crystalline blends which has received a considerable amount of attention is the polymer-dispersed liquid crystal display device. In these systems a low-molecular-weight liquid crystal is dispersed in a polymer matrix. Predictions regarding equilibrium phase behavior are available due to Ballauff[7,8] and Brochard et al.[9,10] The dynamics of thermally induced phase separation in these mixtures was considered by Liu and Fredrickson[11] and the case of polymerization-induced phase separation by Chan and Rey.[12,13]

Most work on the phase separation of truly polymeric liquid crystals, in which no clearing temperature is exhibited, has concentrated on the gelation of isotropic solutions upon cooling. Russo and co-workers have investigated the gelation of poly(γ-benzyl-α-L-glutamate) using video microscopy and light scattering.[14,15] Other groups have also examined gelation in rigid-rod polymer solutions.[16−18] None of these works has investigated the morphology evolution in a thermotropic system quenched into the two-phase region from the nematic phase, presumably due to the lack of an appropriate experimental system. This is unfortunate as liquid crystalline fibers are usually processed from within the nematic phase in the vicinity of the viscosity minimum with respect to concentration.[19]

One system which has been well-characterized experimentally is the blend consisting of poly(ethylene terephthalate) and the main chain copolyester of *p*-hydroxybenzoic acid and ethylene terephthalate.[20,21] Solution casting provides an initially isotropic sample which when heated undergoes phase separation according to an apparent spinodal decomposition mechanism. A characteristic interconnected morphology is present which grows in a self-similar fashion. The present work can explain many of the phenomena demonstrated in such a system.

In this study, a generalized time-dependent Landau−Ginzburg model which treats the kinetics of spinodal decomposition in liquid crystalline mixtures is used to predict morphological trends under various processing conditions. The effects of molecular weight, concentration, temperature, and solvent quality on the phase-separated morphology are all presented. The predictions of the model should prove useful in the design of

* Author to whom correspondence should be addressed.

S0024-9297(97)01204-7 CCC: $15.00
Published on Web 01/13/1998

processing strategies for liquid crystalline fibers and films.

A derivation of the model appears already in the literature,[22] so it is only sketched in the Theory section. More emphasis is placed on the Results and Discussion section in which the characteristic growth factors (eigenvalues) are calculated for a variety of processing conditions, thus allowing the prediction of these effects on morphology; calculated example morphological patterns are also given. In the Conclusions issues regarding the present state-of-the-art in LCP fiber processing are discussed in light of the theoretical predictions.

Theory

The basis of this model is an expression for the equilibrium free energy of a binary mixture of an LCP in a chainlike diluent which allows the explicit calculation of binary phase diagrams and their stability limits.[23,24] This expression is available from a modified version of the lattice theory of the nematic state due to Flory.[25] The resulting free energy is written as an explicit function of composition and a scalar order parameter:

$$\frac{A}{n_0 kT} = -\left[1 - \frac{v_r}{\tilde{V}_r}(1 - y/x_r)\right] \ln\left[1 - \frac{v_r}{\tilde{V}_r}(1 - y/x_r)\right] + \left(\frac{v_r}{x_r \tilde{V}_r}\right) \ln\left(\frac{v_r}{x_r \tilde{V}_r}\right) + \left(\frac{1 - v_r}{x_s \tilde{V}_s}\right) \ln\left(\frac{1 - v_r}{x_s \tilde{V}_s}\right) + \left(\frac{1 - v_r}{x_s \tilde{V}_s}\right)(x_s - 1) + \left(\frac{v_r}{x_r \tilde{V}_r}\right)(y - 1) + \left[1 - \left(\frac{v_r}{\tilde{V}_r} + \frac{1 - v_r}{\tilde{V}_s}\right)\right] \ln\left[1 - \left(\frac{v_r}{\tilde{V}_r} + \frac{1 - v_r}{\tilde{V}_s}\right)\right] - \left(\frac{v_r}{x_r \tilde{V}_r}\right) \ln(x_r y^2) - \left(\frac{v_r^2}{2\theta \tilde{V}_r}\right)\left[\frac{v_r}{\tilde{V}_r} + \frac{1 - v_r}{\tilde{V}_s}\right]\left[1 - \frac{3}{2}\left(\frac{\pi y}{4x_r}\right)^2\right]^2 + \chi v_r \frac{(1 - v_r)}{\tilde{V}_s} \quad (1)$$

where A is the Helmholtz free energy, n_0 is the number of sites on the lattice, k is Boltzmann's constant, T is temperature, v_r is the volume fraction of the liquid crystalline component, y is the scalar-valued Flory order parameter, θ is the reduced temperature, χ is the usual Flory energetics interaction parameter, and x_r represents the aspect ratio of the rigid liquid crystalline molecule while x_s represents the contour length of the chainlike solvent, and $\tilde{V}_r$ and $\tilde{V}_s$ represent the reduced volume of the two components, respectively.

When the contour length of the chainlike solvent is set equal to 1, the system corresponds to an LCP in solution. An example equilibrium temperature−composition phase diagram for this situation is given in Figure 1; the ordinate is θ, the reduced temperature, and the abscissa is v_r, the volume fraction of LCP. The mixture is isotropic at low concentrations but beyond a critical concentration a biphasic region appears and a nematic phase is present in equilibrium with the isotropic phase. Further increases in concentration lead to the entire mixture becoming ordered as a nematic phase. The equilibrium boundaries between isotropic and nematic phases (the binodal curves) contain the

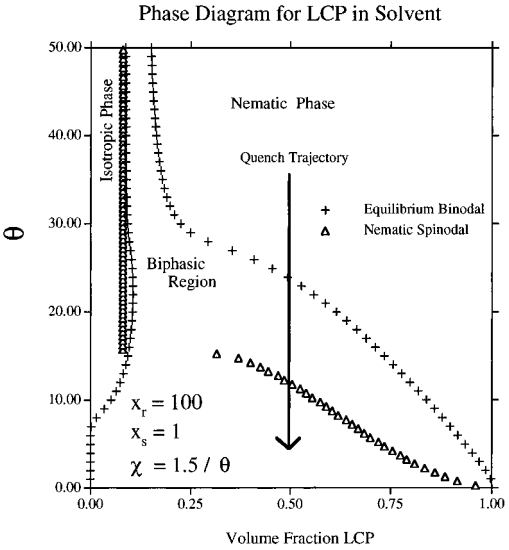

Figure 1. Equilibrium phase diagram for a nematic LCP in solution. The binodal (+) and nematic spinodal (△) are shown along with a typical quench trajectory.

biphasic region—as the temperature is lowered the width of the biphasic region increases so that at the lowest temperatures a pure polymer ($v_r = 1.0$) nematic phase is in equilibrium with a pure solvent ($v_r = 0.0$) isotropic phase. Also shown is a typical quench trajectory from the stable nematic phase into the two-phase region beneath the spinodal curve. Further details about such phase diagrams can be found in an earlier work.[24]

To construct a dynamic theory, the equilibrium free energy is used as the basis for a free energy functional which can include the effects of inhomogeneities. The free energy is converted into a free energy density by dividing by the volume of an elementary lattice site, v_0*:

$$F = \frac{A}{n_0 v_0^* kT} \quad (2)$$

Next, the effects of the inhomogeneities are accounted for by expanding in the variations and their gradients; the resulting functional is

$$f = \int_V \frac{1}{2}\left[\left(\frac{\partial^2 F}{\partial v_r^2}\right)(v_r - v_{r,0})^2 + \left(\frac{\partial^2 F}{\partial y^2}\right)(y - y_0)^2 + \left(\frac{\partial^2 F}{\partial v_r \partial y}\right)(v_r - v_{r,0})(y - y_0)\right] + \kappa(\nabla(v_r - v_{r,0}))^2 + \eta(\nabla(y - y_0))^2 \, dx \, dy \, dz \quad (3)$$

where the initial homogeneous state of the material is denoted as y_0 and $v_{r,0}$, κ and η are the interfacial gradient energy parameters, and the integration is over the sample volume.

The usual Landau−Ginzburg reasoning applied to the free energy functional yields a dynamic model which is consistent with model C in the well-known classification scheme of Hohenberg and Halperin.[26] In the present case the volume fraction of liquid crystal, v_r, serves as the conserved quantity while the Flory order parameter, y, is the nonconserved quantity. The linearized forms

of the resulting dynamic equations are:

$$\frac{\partial v_r}{\partial t} = M\left\{\left(\frac{\partial^2 F}{\partial {v_r}^2}\right)\nabla^2(v_r - v_{r,0}) - 2\kappa\nabla^4(v_r - v_{r,0})\right\} + M\left\{\left(\frac{\partial^2 F}{\partial v_r \partial y}\right)\nabla^2(y - y_0)\right\} \quad (4)$$

$$\frac{\partial y}{\partial t} = -R\left\{\left(\frac{\partial^2 F}{\partial y^2}\right)(y - y_0) - 2\eta\nabla^2(y - y_0)\right\} - R\left\{\left(\frac{\partial^2 F}{\partial v_r \partial y}\right)(v_r - v_{r,0})\right\} \quad (5)$$

where M and R are phenomenological coefficients related to the translational and rotational diffusivities. In order to describe the phase separation process, the derivative terms of the free energy density must be evaluated at the quench conditions. It is of interest to note that if the coupling term involving the mixed derivative is set equal to zero, then eq 4 reduces to the linearized Cahn−Hilliard equation for spinodal decomposition in isotropic materials.[27]

Fourier methods may be used to solve the system of linearized equations; transformation of the spatial dependence yields a set of coupled first-order ordinary differential equations for which an analytical solution is available. The forms of the solutions are

$$v_\beta = C_1(\beta)\exp\{\lambda_1(\beta)t\} + C_2(\beta)\exp\{\lambda_2(\beta)t\} \quad (6)$$

$$y_\beta = C_3(\beta)\exp\{\lambda_1(\beta)t\} + C_4(\beta)\exp\{\lambda_2(\beta)t\} \quad (7)$$

in which β is the Fourier wavenumber and the transformed variables are y_β and v_β. The coefficients C_1−C_4 are accurately reported in an earlier work while the correct expressions (compare ref 22) for the eigenvalues $\lambda_1(\beta)$ and $\lambda_2(\beta)$ are

$$\lambda_1(\beta) = -\frac{1}{2}\left\{R\left[\left(\frac{\partial^2 F}{\partial y^2}\right) + 2\eta\beta^2\right] + M\beta^2\left[\left(\frac{\partial^2 F}{\partial {v_r}^2}\right) + 2\kappa\beta^2\right]\right\} + \frac{1}{2}\left\{\left(R\left[\left(\frac{\partial^2 F}{\partial y^2}\right) + 2\eta\beta^2\right] - M\beta^2\left[\left(\frac{\partial^2 F}{\partial {v_r}^2}\right) + 2\kappa\beta^2\right]\right)^2 + 4MR\beta^2\left[\left(\frac{\partial^2 F}{\partial v_r \partial y}\right)^2\right]\right\}^{1/2} \quad (8)$$

and

$$\lambda_2(\beta) = -\frac{1}{2}\left\{R\left[\left(\frac{\partial^2 F}{\partial y^2}\right) + 2\eta\beta^2\right] + M\beta^2\left[\left(\frac{\partial^2 F}{\partial {v_r}^2}\right) + 2\kappa\beta^2\right]\right\} - \frac{1}{2}\left\{\left(R\left[\left(\frac{\partial^2 F}{\partial y^2}\right) + 2\eta\beta^2\right] - M\beta^2\left[\left(\frac{\partial^2 F}{\partial {v_r}^2}\right) + 2\kappa\beta^2\right]\right)^2 + 4MR\beta^2\left[\left(\frac{\partial^2 F}{\partial v_r \partial y}\right)^2\right]\right\}^{1/2} \quad (9)$$

In discussing phase separation, the eigenvalues are referred to as amplification factors because for positive values the compositional and orientational fluctuations will grow exponentially as time progresses according to eqs 6 and 7. Negative eigenvalues mean that fluctuations die away as time increases.

Table 1. Parameter Values for Model Calculations

$\kappa = 1.25 \times 10^{-11}$ 1/m	$\eta = 4.65 \times 10^{-12}$ 1/m
$\tau_{RELAX} = 1.18 \times 10^{-2}$ s	$D_{TRANS} = 3.09 \times 10^{-11}$ m²/s
$x_r = 100$	$x_s = 1$

The amplification factors contain all of the information about how the morphology of the phase-separating system will evolve within the linear regime. This is because there exists a corresponding real space length scale associated with each wavenumber β. The relationship between this length scale and the wavenumber is given by

$$\beta = \frac{2\pi}{\Lambda} \quad (10)$$

where Λ is the real space length scale. The magnitude of the amplification factor in a plot versus the wavenumber reflects the strength of the fluctuations on a length scale related to the wavenumber through eq 10. If either of the amplification factors is positive for a given wavenumber, the system will phase separate into domains of the corresponding size.

In order to compare the theoretical predictions directly with patterns observed in a polarizing microscope, the linear equations are also solved in two spatial dimensions using a finite difference scheme. Equations 4 and 5 are solved in a dimensional representation in order to facilitate the comparison of predicted domain sizes with experimental observation. The fourth-order terms are evaluated using a next nearest neighbor representation; this provides second order accuracy in the grid spacing. Simulations are performed on a 100 × 100 grid with the imposition of periodic boundary conditions in both directions; the box length corresponds to 5 μm in real space dimensions. The initial value problem is solved in FORTRAN using the May 1994 version of VODPK (variable-coefficient ordinary differential equation package with preconditioned Krylov method for the solution of linear systems) due to Byrne, Brown, and Hindmarsch.[28,29]

Results and Discussion

Consider the case of isothermal aging whereby the nematic phase is brought suddenly into the spinodal regime of the phase diagram and held at a constant temperature. Such a situation is depicted on the phase diagram of Figure 1. The appropriate initial conditions for the dynamic model consist of small fluctuations in the values of v_r and y that are present in the material before being brought to within the spinodal. Specification of the initial position on the phase diagram fixes the initial values for the composition and reduced temperature, allowing the calculation of the initial value for the orientational order parameter. Given a quench temperature within the spinodal region of the phase diagram and values for the phenomenological coefficients, the amplification factors can be calculated. The parameter values used in the calculations are given in Table 1 for the quench shown in Figure 1.

The trajectory shown in Figure 1 consists of a temperature quench from a high-temperature stable nematic phase into the low-temperature unstable biphasic region. For this case, plots of the amplification factors as a function of the wavenumber are shown in Figures 2 and 3. The high-temperature case is shown in Figure 2; both amplification factors are negative for all values of the wavenumber β. Thus, at this temperature no

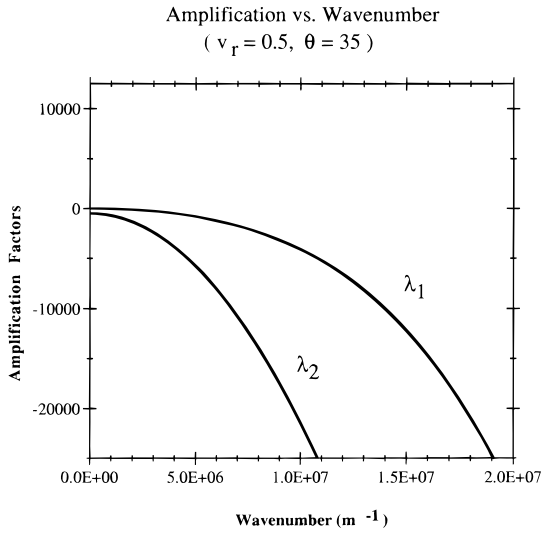

Figure 2. Values of the amplification factors in the stable nematic phase. Both amplification factors are negative, implying that fluctuations are stable and that spinodal decomposition does not occur.

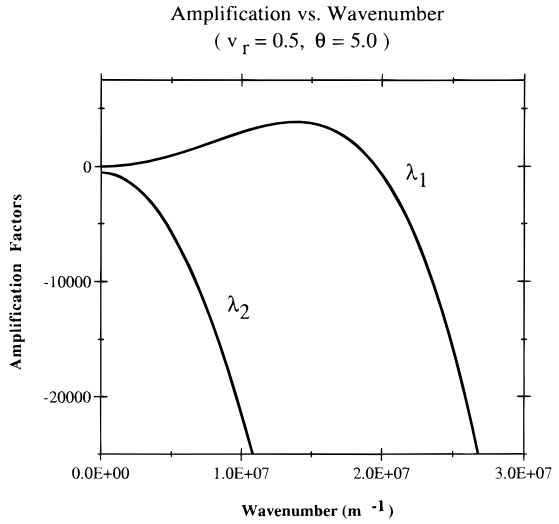

Figure 3. Values of the amplification factors for a quench into the spinodal. The first amplification factor, λ_1, exhibits a well-defined maximum, implying phase separation by a spinodal mechanism.

fluctuations are amplified and the material remains homogeneous for all times. The amplification factors evaluated at the quenching temperature are shown in Figure 3. It is seen that there is a well-defined maximum in λ_1, the first amplification factor, which is positive over a limited range before passing through zero and becoming negative. Values of the wavenumber at which the maximum occurs ($\beta_{max} \approx 1.4 \times 10^7$ 1/m) correspond to real space domains of about 0.45 μm according to eq 10. The second amplification factor is always found to be negative for all values of the wavenumber.

Morphological evolution for the quenched material is elucidated in Figure 4 which gives patterns for both the concentration and the order parameter at different times. The initial conditions are calculated as randomly fluctuating with the use of a random number generator called at each grid point; the magnitude of the fluctuation is taken as the reciprocal of the respective second derivative as dictated by the fluctuation dissipation theorem.[22] In addition, the 5-fold decrease in absolute temperature leads to the supression of the order parameter fluctuations upon quenching. At very early times (0.1 ms) the order parameter pattern is not coincident with the composition, but as time progresses the two scalar fields do converge to the same spatial mapping. This finding is consistent with earlier results from the analytical model and can be interpreted to mean that the molecular order is necessarily strongly coupled to the concentration field. It is physical to expect that the spatial regions of high molecular order are necessarily the same regions which contain high concentrations of the LCP.

Like the Cahn theory for isotropic media, the present model predicts the existence of a bicontinuous interconnected morphology. In addition, the present theory is capable of describing the spatial evolution of the order parameter and predicts reasonable length scales for macromolecular materials (i.e., on the order of microns). However, it is important to realize the limitations of these calculations. Only the linearized version of the model is being solved, so no change in the domain size with time is predicted. In reality, the morphology will coarsen and become larger in a self-similar fashion; coarsening behavior can only be captured by solving the fully nonlinear version of the model. Even then, the model is too coarse grained to provide any information about the actual director field; nothing can be said about the existence of disclinations within the spatially distributed nematic phase. Despite these limitations, the

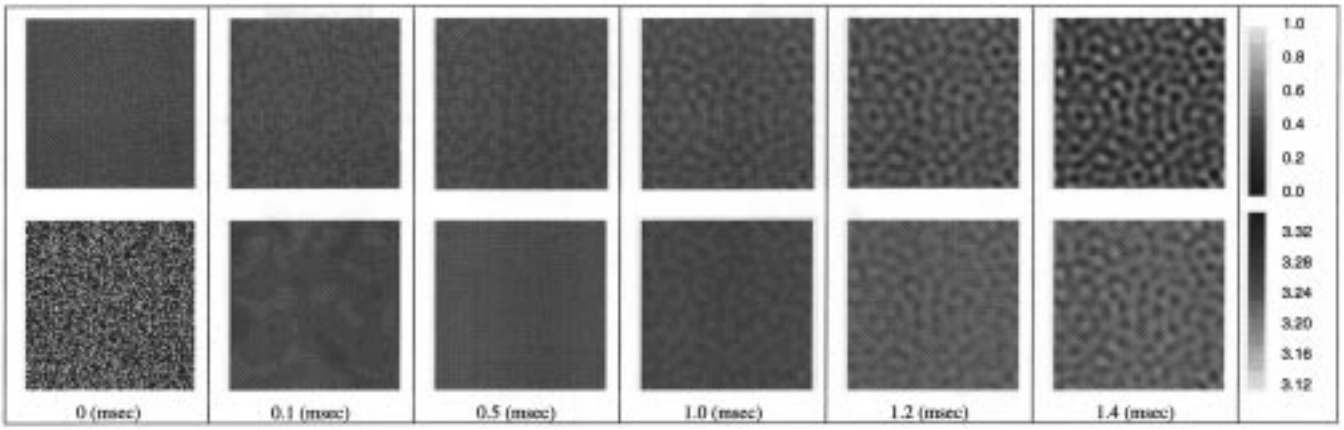

Figure 4. Time evolution of the order and concentration fields. Initially, the material is at $\theta = 35$, $v_r = 0.5$, and $y = 3.23$ but is quenched to at $\theta = 5$. The early time order parameter pattern is suppressed due to coupling to the concentration field (see text for details).

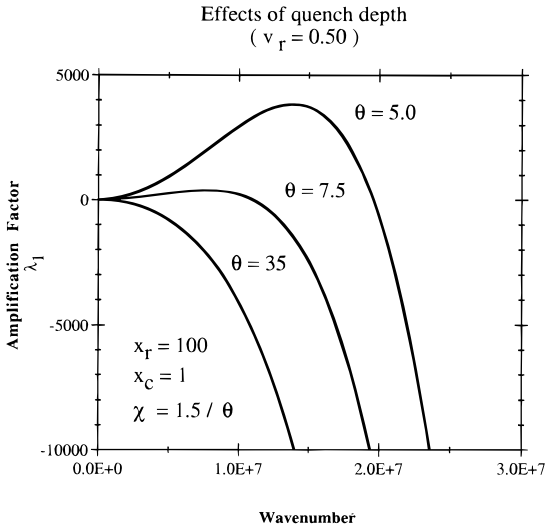

Figure 5. Effect of quench depth. As the quench temperature is reduced to lower values, the maximum in the amplification factor occurs at larger wavenumbers, meaning smaller domains are formed.

theoretical predictions in the linear regime are in accordance with recent experimental studies using video microscopy.[21]

Processing effects, like quench depth beneath the spinodal, on the length scale of phase separation can be examined within the context of the model. In Figure 5, the first amplification factor is given for $v_r = 0.50$ and the stable reduced temperature of $\theta = 35.0$ as well as for the unstable temperatures of $\theta = 7.5$ and 5.0. These calculations again correspond to the phase diagram of Figure 1. It is clearly demonstrated that as the quench temperature is reduced from 7.5 to 5.0, the maximum value of the amplification factor shifts to larger wavenumbers. This implies that deeper quenches result in smaller domains, a finding which is consistent with theories of phase separation in isotropic media.

Figure 6 provides a comparison of the order parameter and concentration patterns for the two different temperatures; in this representation it is particularly facile to see that deeper quenches do indeed produce smaller domains. It is also apparent that, in order to reach comparable degrees of phase separation, the shallower quench requires a greater amount of time (roughly 16 vs 1 ms). This is not surprising given the greater width of the two-phase region at lower temperatures—the distance from the equilibrium is a measure of the available driving force for phase separation. The greater this driving force, the faster phase separation proceeds. An interesting observation is that the shallower quench produces a higher degree of orientation (lower value of the Flory order parameter) in the nematic rich phase. This phenomena is presumably attributable to the ability of the material to orientationally relax on the slower time scale of the shallow quench.

Figure 7 illustrates the effect of LCP concentration on domain size. The calculations correspond to the phase diagram of Figure 1, but in this case three different initial concentrations are considered. In all cases the initial temperature is taken as $\theta = 35.0$ and the quench temperature is $\theta = 5.0$; the rotational

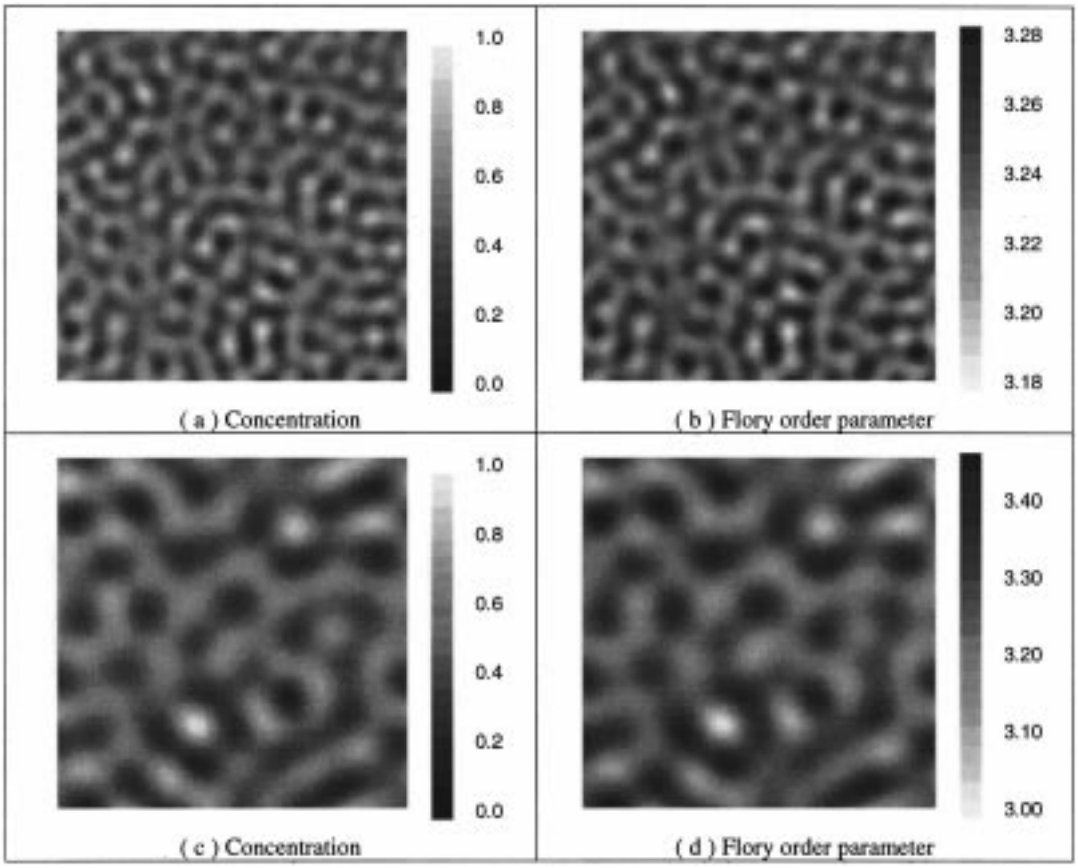

Figure 6. Morphology of differently quenched samples. The results in (a) and (b) are for a sample initially at $\theta = 35$, $v_r = 0.5$, and $y = 3.23$ quenched to $\theta = 5$ for 1.4 ms; (c) and (d) correspond to a quench of $\theta = 7.5$ held for 16.0 ms. A higher degree of molecular orientation is achieved in the more slowly phase-separating case.

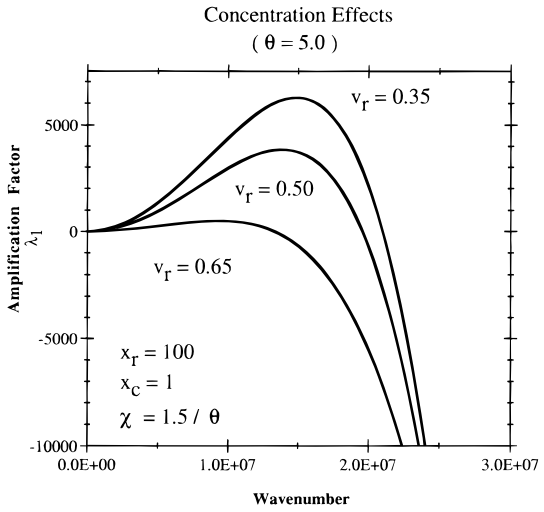

Figure 7. Effect of concentration. The samples are initially at $\theta = 35$ and are quenched to $\theta = 5$; volume fractions are given in the figure. As the concentration of the LCP is increased, the maximum in the amplification factor occurs at lower wavenumbers, meaning larger domains are formed.

diffusivity is scaled according to $D_r \propto v_r^{-2}$ by adjusting the value of the coefficient R. The calculations demonstrate that as the concentration is increased, the domain size becomes larger; this represents a unique prediction of the model. This behavior is attributable to the absence of a critical point in the LCP phase diagram—unlike isotropic solutions there is no point of symmetry with respect to the domain formation. Corresponding patterns are given in Figure 8 for the cases of $v_r = 0.35$ and 0.65. Comparison may also be made with Figure 6a,b for the $v_r = 0.50$ case. Both the amplification factor plot of Figure 7 and the morphology patterns demonstrate that the domain size to concentration relationship is not linear; the same concentration change of $\Delta v_r = 0.15$ produces a much greater effect between $v_r = 0.50$ and 0.65 than it does between between $v_r = 0.35$ and 0.50. This prediction is one of the most important findings of the present investigation and has direct relevance toward LCP processing issues.

Another important processing consideration is solvent quality, and this can also be examined within the context of the present model by varying χ, the energetics parameter. Changes in the phase diagram with increasing χ include a widening of the two-phase region and the onset of phase separation at a higher temperature; details of these changes are given in an earlier article.[24] For the present purposes, the amplification factor is calculated for the same LCP as above but for differing values of the energetics parameter—results are presented in Figure 9. Raising χ is equivalent to decreasing the solvent quality (poorer solvation), and the calculations suggest that this leads to a maximum in the amplification factor at greater values of the wavenumber. That is to say, the use of a poorer solvent will have the effect of decreasing the domain size.

A final material parameter which can be investigated is the LCP molecular weight. The details of changes in the phase diagrams are also given in the earlier article.[24] The morphological considerations are evident in Figure 10 which demonstrates that as the aspect ratio of the LCP is increased from 25 to 100, the wavenumber

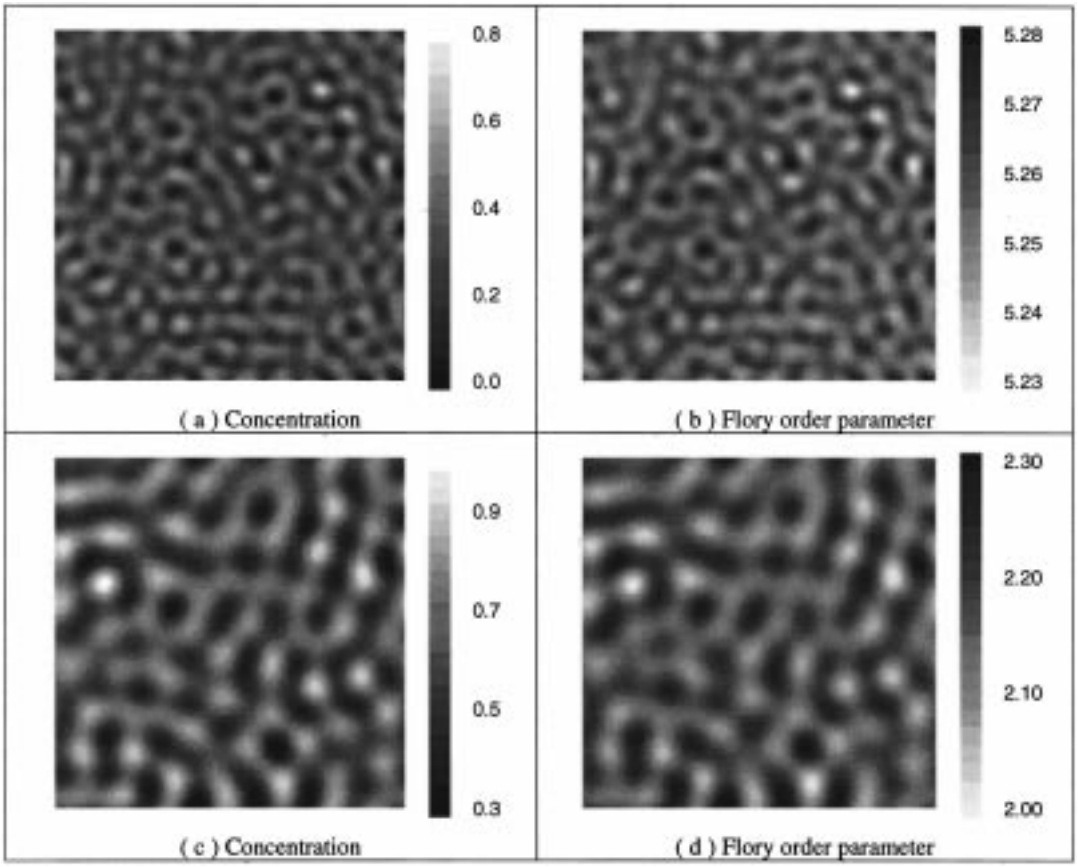

Figure 8. Morphology of different concentrations. The results in (a) and (b) are for a sample initially at $v_r = 0.35$, $y = 5.26$, and $\theta = 35$ quenched to $\theta = 5$ for 0.8 ms; (c) and (d) correspond to a sample initially at $v_r = 0.65$, $y = 2.15$, and $\theta = 35$ quenched to $\theta = 5$ for 12.5 ms. Increasing concentration leads to larger domain sizes.

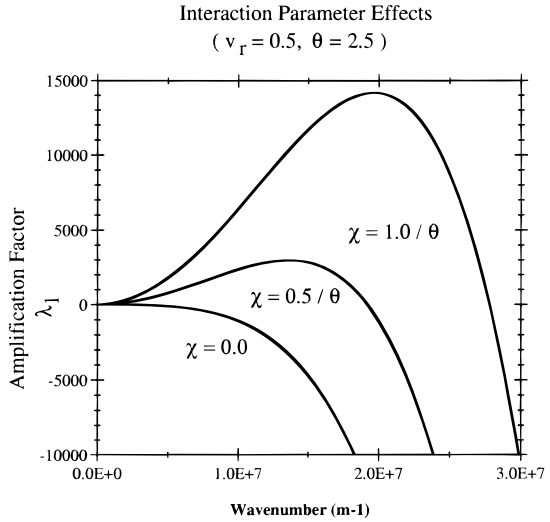

Figure 9. Effect of the interaction parameter. As the interaction parameter increases, the maximum in the amplification factor occurs at higher wavenumbers, meaning smaller domains are formed. The sample is initially at $\theta = 35$ and $v_r = 0.5$ and then are quenched to $\theta = 2.5$; values for the interaction parameter are given in the figure.

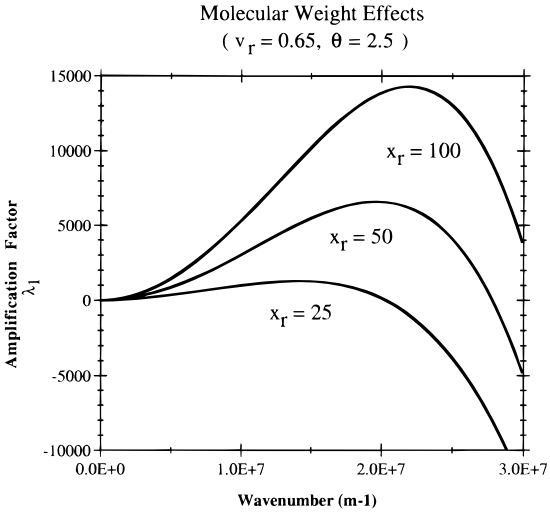

Figure 10. Effect of LCP molecular weight. For the same processing conditions, increasing the molecular weight leads to the maximum in the amplification factor shifting to higher wavenumbers, meaning smaller domains are formed. The samples are initially at $\theta = 35$ and $v_r = 0.65$ and then are quenched to $\theta = 2.5$; values for the LCP aspect ratios are given in the figure.

at which the amplification factor is a maximum changes from 1.4×10^7 to 2.2×10^7 m^{-1}. Thus increases in molecular weight cause a decrease in the domain size for phase separation during spinodal decomposition in LCPs.

Conclusions

Analytical and computational results from a Landau−Ginzburg model which treats the problem of simultaneous phase separation and ordering for LCPs in solution are presented. The time evolution of one conserved order parameter (polymer volume fraction) and one nonconserved order parameter (the Flory orientational order parameter) is considered. Processing effects including quench temperature, composition, solvent quality, and molecular weight are considered. Growth factors as well as numerical calculations are presented in order to elucidate how the morphology of the system is influenced by these processing effects.

Within the framework of the model, several predictions regarding the effects of different processing strategies on phase-separated morphologies are available. In particular, simulations of example quenching experiments demonstrate that increased LCP concentration, decreased molecular weight, increased solvation, and decreased quench depth all lead to increased domain size.

These results are suggestive of optimal LCP processing strategies to achieve the best all around mechanical properties. Generally, high molecular mass is advantageous for properties, but in this case it will lead to smaller domains and therefore more microfibrillar interfacial area per unit material. In the case of LCP fibers, increasing molecular weight may increase tensile properties at the expense of compressive properties. Shallow quenches from good solvents are expected to produce materials with both larger domain sizes and greater degrees of molecular orientation.

The present model addresses the case of a rigid rod undergoing a thermal quench while most LCP fiber processing involves the coagulation of a lyotropic solution by a nonsolvent. In the limit of fast mass transfer, the trends of the processing effects might be similar. Generally, lyotropic LCPs are processed from solutions having as high a molecular weight as possible and in the vicinity of the viscosity minimum with respect to concentration. The results of the present calculations imply that if the reduction of microfibrillar interfacial area is a route toward better compressive properties, then there is an incentive for spinning fibers and casting films from higher concentration solutions with reduced molecular weight materials.

Acknowledgment. This work was supported by a Faculty Early Career Development Grant, CTS-9502466, from the National Science Foundation. Helpful suggestions regarding the numerical aspects of the study were made by Professor Erik van Vleck of the CSM Mathematics and Computer Science Department.

References and Notes

(1) Krause, S. J.; et al. *Polymer* **1988**, *29*, 1356.
(2) Allen, S. R.; Farris, R. J.; Thomas, E. L. *J. Mater. Sci.* **1985**, *20*, 2727.
(3) Allen, S. R.; Farris, R. J.; Thomas, E. L. *J. Mater. Sci.* **1985**, *20*, 4583.
(4) Deteresa, S. J., Ed.; University of Massachusetts: Amherst, 1985.
(5) Cohen, Y.; Thomas, E. L. *Macromolecules* **1988**, *21*, 433.
(6) Epstein, A. J.; Yang, Y. *MRS Bull.* **1997**, June.
(7) Ballauff, M. *Mol. Cryst. Liq. Cryst.* **1986**, *136*, 175.
(8) Dorgan, J. R.; Soane, D. *Mol. Cryst. Liq. Cryst.* **1990**, *188*, 129.
(9) Brochard, F.; Jouffroy, J.; Levinson, P. *J. Phys.* **1984**, *45*, 1125.
(10) Kyu, T.; Chiu, H. *J. Chem. Phys.* **1995**, *103*, 7471.
(11) Liu, A. J.; Fredrickson, G. *Macromolecules* **1996**, *29*, 8000.
(12) Chan, P. K.; Rey, A. D. *Macromolecules* **1996**, *29*, 8934.
(13) Chan, P. K.; Rey, A. D. *Macromolecules* **1997**, *30*, 2135.
(14) Chowdhury, A. H.; Russo, P. S. *J. Chem. Phys.* **1990**, *92*, 5744.
(15) Tipton, D. L.; Russo, P. S. *Macromolecules* **1996**, *29*, 7402.
(16) Jackson, C. L.; Shaw, M. T. *Polymer* **1990**, *31*, 1070.
(17) Kyu, T.; Mukherjee, P. *Liq. Cryst.* **1988**, *3*, 631.
(18) Kyu, T.; Yang, J.; Cheng, S. Z.; Hsu, S. L. C.; Harris, F. W. *Macromolecules* **1994**, *27*, 1861.

(19) Acierno, D.; Collyer, A. A. *Rheology and Processing of Liquid Crystal Polymers*; Chapman and Hall: London, 1996.
(20) Nakai, A.; Shiwaku, T.; Hasegawa, H.; Hashimoto, T. *Macromolecules* **1986**, *19*, 3008.
(21) Nakai, A.; Shiwaku, T.; Wang, W.; Hasegawa, H.; Hashimoto, T. *Macromolecules* **1996**, *29*, 5990−6001.
(22) Dorgan, J. R. *J. Chem. Phys.* **1993**, *98*, 9094.
(23) Dorgan, J. R. *Liq. Cryst.* **1991**, *10*, 347.
(24) Dorgan, J. R. *Fluid Phase Equilib.* **1995**, *109*, 157.
(25) Flory, P. J. *Proc. R. Soc. London* **1956**, *234*, 73.
(26) Hohenberg, P. C.; Halperin, B. I. *Rev. Mod. Phys.* **1977**, *49*, 435.
(27) Cahn, J. W. *Trans. Metall. Soc. AIME* **1968**, *242*, 166.
(28) Brown, P. N.; Byrne, G. D.; Hindmarsch, A. C. *SIAM J. Sci. Stat. Comput.* **1989**, *10*, 1038.
(29) Brown, P. N.; Hindmarsch, A. C. *J. Appl. Math. Comput.* **1989**, *31*, 40.

MA971204B